X-ray rocking curve study of Si-implanted GaAs, Si, and Ge

V. S. Speriosu,[a] B. M. Paine, and M-A. Nicolet
California Institute of Technology, Pasadena, California 91125

H. L. Glass
Rockwell International, Microelectronics Research and Development Center, Anaheim, California 92803

(Received 6 November 1981; accepted for publication 8 January 1982)

Crystalline properties of Si-implanted ⟨100⟩ GaAs, Si, and Ge have been studied by Bragg case double-crystal x-ray diffraction. Sharp qualitative and quantitative differences were found between the damage in GaAs on one hand and Si and Ge on the other. In Si and Ge the number of defects and the strain increase linearly with dose up to the amorphous threshold. In GaAs the increase in these quantities is neither linear nor monotonic with dose. At a moderate damage level the GaAs crystal undergoes a transition from elastic to plastic behavior. This transition is accompanied by the creation of extended defects, which are not detected in Si or Ge.

PACS numbers: 61.10.Fr, 61.70.Tm, 62.20.Fe

The existence of different annealing behavior in ion-implanted amorphized GaAs compared to Si and Ge has been known for some time. In Si and Ge layer regrowth is linear with time and there is good epitaxy.[1–3] In GaAs layer regrowth is nonlinear with time[4] and, independently of ion species, epitaxy is poor.[5] To obtain good electrical activity, implantation in Si and Ge is done at room temperature with doses sufficient to amorphize the material.[6] In GaAs the temperature is held at a few hundred °C in order to prevent amorphization of the layer.[7] Up to the present no substantive evidence has been published concerning the cause of these differences. In this letter we present an x-ray diffraction study of Si-implanted ⟨100⟩ GaAs, Si, and Ge. The results indicate that the evolution of the damage up to amorphousness in GaAs is very different from that in Si and Ge.

⟨100⟩-oriented GaAs, Si, and Ge single crystals, about 5 mm × 5 mm × 0.5 mm in size, highly polished, were implanted with 300-keV Si^+ (in GaAs and Ge) and 230-keV Si^+ (in Si). Implantation was done at room temperature (RT) with a current density of 0.125 μA/cm^2 and under conditions excluding channeling. Doses ranged from 1×10^{13} atom/cm^2 to 1.2×10^{15} atom/cm^2 for GaAs, 1×10^{13} atom/cm^2 to 7×10^{13} atom/cm^2 for Ge, and 7×10^{13} atom/cm^2 to 7×10^{14} atom/cm^2 for Si. These doses produced modifications in crystal structure measurable by Bragg case double-crystal x-ray diffraction. Well-collimated, low-divergence Fe K_α x rays were obtained with symmetric (400) reflections from nearly perfect ⟨100⟩ monochromators (GaAs for the GaAs and Ge samples, Si for the Si samples). The spot size at the sample was limited to ~1 mm × 1 mm by a set of slits. Typical counting rate for the beam incident on the sample was $\sim10^5$ cps. The diffracted intensity (reflecting power) as a function of angle was measured with a NaI(Tl) detector with pulse height analysis.

Representative diffraction profiles (rocking curves) for the three crystals are shown in Fig. 1. Only the low-angle side of the virgin crystal's Bragg peak is shown. The high-angle side is little changed by implantation. The virgin peak at zero angle, also not shown, is 10 to 100 times more intense than the oscillatory structures shown in the figure. The behavior of the rocking curve with increasing dose for Si [Fig. 1(a)] is similar to that for Ge [Fig. 1(b)]. For both crystals the angular range of nonzero reflecting power increases linearly with dose, the peak farthest from zero angle decreases in relation to other peaks, and the overall reflecting power diminishes. At the highest doses the reflecting power approaches the curve obtained with virgin crystal, indicating that the implanted layer is nearly amorphous. Pronounced

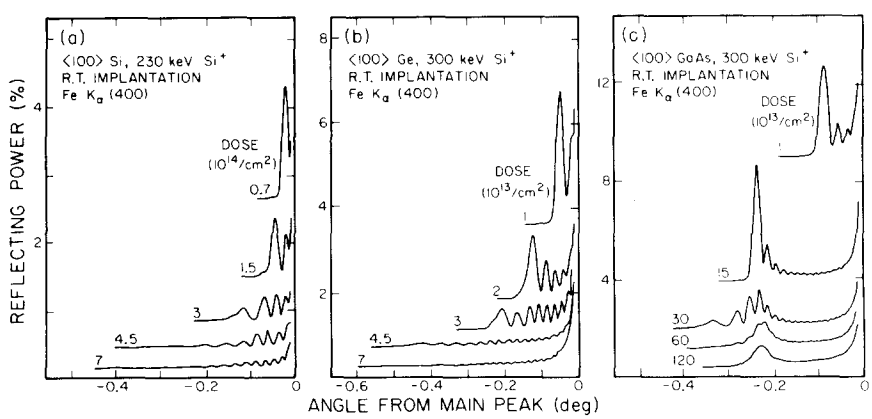

FIG. 1. Rocking curves corresponding to several doses for (a) Si, (b) Ge, and (c) GaAs. The angle is referred to the location of the Bragg peak of virgin crystal. The curves are vertically displaced for clarity. For each curve zero reflecting power occurs at the lowest angle for which the curve is plotted.

[a]IBM predoctoral fellow.

 0003-6951/82/070604-03$01.00

oscillations are maintained over the entire range of doses. The behavior of the GaAs rocking curves [Fig. 1(c)] is very different. As the dose is varied by two orders of magnitude, the range of nonzero reflecting power changes by only a factor of 3. Between 1×10^{13} atom/cm^2 and 1.5×10^{14} atom/cm^2 the principal peak becomes narrower and more intense. Between 1.5×10^{14} atom/cm^2 and 3.0×10^{14} atom/cm^2 the rocking curve broadens, but its shape is different from any obtained in Si or Ge. For doses above 6.0×10^{14} atom/cm^2 the oscillations are smoothed out, although, as indicated by the single peak for the 1.2×10^{15} atom/cm^2 dose, the implanted layer is not amorphous.

The rocking curves of Fig. 1 have been interpreted with the aid of a kinematical model of x-ray diffraction in crystals.[8] The model generates rocking curves for arbitrary depth-dependent distributions of strain, point defects and extended defects. The category of point defects includes individual random atomic displacements as well as highly distorted regions extending over a small number (i.e., one to ten) of unit cells. The category of extended defects covers imperfections that generate small lattice distortions extending over many (i.e., hundreds of) unit cells. Detailed distributions for the strain and the two types of defects are obtainable by fitting experimental rocking curves. The trail-and-error fitting procedure must be performed on a computer. However, several useful parameters are readily found directly from the rocking curve.[8] The total thickness T of the damaged layer is obtained from the most rapid oscillation in the rocking curve, and the maximum strain ϵ_{max} is linearly related to the angle where the rocking curve rises from zero reflecting power.[8] The estimated accuracy for T and ϵ_{max} obtained in this manner is 5%. The number of point defects can be obtained by comparing the areas under rocking curves of damaged and perfect crystals of the same thickness T. Similarly, the presence of extended defects and estimates for their size, amount of random misorientation, and lateral variation of strain are obtainable from the degree of smoothing of the rocking curve.[8,9]

The thickness of the damaged layer is 5200 Å for Si and 5800 Å for Ge and GaAs. Figure 2 shows the maximum strain as a function of dose for the three crystals. Also included is a line of slope one. The maximum strain below the amorphous threshold is around 1% for all three crystals. For Si and Ge, the maximum strain and, by implication, the entire strain distribution, increase nearly linearly with dose. The data for Si and Ge indicate that the number of point defects, describable by a Debye–Waller factor,[8] also increases nearly linearly with dose. Extended defects, as defined above, are absent up to the amorphous threshold.

In GaAs the maximum strain as a function of dose is much more complicated. Here the strain curve can be subdivided into five different regions, as indicated in the figure. Below 10^{13} atom/cm^2 (region I) the strain is assumed to rise linearly with dose. Between 10^{13} atom/cm^2 and $\sim10^{14}$ atom/cm^2 (region II) pronounced saturation sets in. The saturation occurs not only in the maximum strain, but in the entire strain distribution. This is indicated in Fig. 1(c) by the greater sharpness of the principal peak for 1.5×10^{14} atom/cm^2 compared to that for 1×10^{13} atom/cm^2. In region III, between 1×10^{14} atom/cm^2 and 3×10^{14} atom/cm^2, there is a sharp rise in the maximum strain. Between 3×10^{14} atom/cm^2 and $\sim1.2\times10^{15}$ atom/cm^2 (region IV) the maximum as well as the entire strain distribution no longer change with dose. For higher doses (region V) the layer approaches amorphousness. From region I through III, the number of point effects increases with the strain. In region IV it is not clear whether net point defects continue to be created. Instead, extended defects become observable, their density increasing with dose and reaching a value of $\sim1/\mu m^2$ at 1.2×10^{15} atom/cm^2. The rocking curve contains very little information concerning the detailed structure of these extended defects. All that can be said is that they extend throughout most of the implanted layer thickness; the lateral variation in strain is not more than 0.01%, and the variation in orientation is less than ~2 arc min. Attempts to observe the extended defects through x-ray topography have not been successful, probably due to the small variation in orientation compared to the width of the rocking curve.

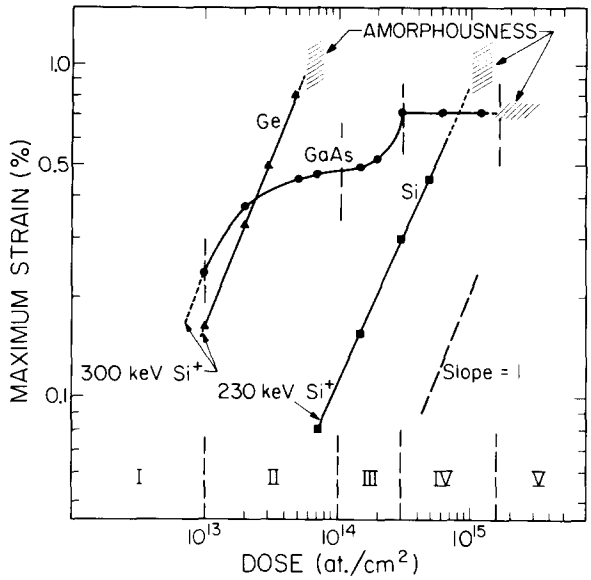

FIG. 2. Maximum strain as a function of dose for Si, Ge, and GaAs. The five dose regions apply to the strain in GaAs.

The mechanism of strain creation in ion-implanted crystals is not very well understood. It has been shown[10] that in garnets the strain distribution is proportional to the energy deposited through nuclear collisions during implantation. It has also been shown[8] that in garnets the strain and damage distributions are proportional to each other. The implanted lattice is constrained by the underlying undamaged crystal to expand only in a direction perpendicular to the surface.[8] This places the implanted layer in lateral compression[11] and gives a Poisson contribution to the strain. As indicated in Fig. 2, for the same strain the dose in Si is about 20 times larger than in Ge. However, the rocking curves show that in both crystals comparable strains correspond to comparable numbers of point defects.

In GaAs pronounced annealing during implantation occurs in region II of Fig. 2. In region III the average strain

reaches its yield value of 0.45%. This number is nearly equal to that obtained[12] for the tensile yield strain of undamaged, externally stressed ⟨110⟩ GaAs. In virgin GaAs the onset of plastic deformation is accompanied by the abrupt creation of 60° dislocations.[12] In lattice-mismatched, epitaxially grown layers, misfit dislocations begin to appear when it is energetically favorable to decrease the macroscopic (coherent) strain at the expense of creating localized distortions.[13] The threshold (yield) strain depends, among other things, on the layer thickness as well as on the depth distribution of the strain.[14]

In region IV of Fig. 2 the strain in GaAs no longer changes with the dose. This is perhaps due to a combination of annihilation of point defects at sinks such as extended defects and/or to the relaxation of strict lattice match with the underlying crystal. The deposited energy goes into the creation of extended defects whose density increases with the dose.

The results presented above imply a different structure of the damaged layer for amorphized GaAs compared to Si and Ge. This difference can explain the observed differences in annealing behavior. For Si and Ge, starting at the deep end of the damage deposition curve, the elastic strain and the number of point defects rise uniformly up to the amorphous threshold.[15] With this structure one expects that, during post-implantation annealing, the regrowth is layer by layer using the good seed at the deep end of the damge, thus resulting in relatively good epitaxy.

In GaAs the implanted layer consists of three regions. At the deep end of the damage the strain is elastic and only point defects are present. Between the elastically strained and amorphous regions is a plastically deformed region. This region, containing extended defects, will present a barrier to epitaxial regrowth. The existence of this barrier depends on whether or not the yield strain is reached, regardless of how it is reached. Thus the regrowth of the amorphized layer will be independent of the implanted ion species, as observed.[5] At elevated implantation temperatures, the rate of self-annealing is probably sufficiently high such that for all doses the strain will remain below the yield value (regions I and II of Fig. 2). Thus the plastically deformed region does not develop. It is probably for this reason that elevated temperature implantations of dopants in GaAs give best regrowth and electrical properties.[7] For room-temperature implantation, the elastically strained portion of the layer will regrow epitaxially. It is in fact observed that amorphized GaAs layers show an initial epitaxial regrowth at the buried crystal/amorphous interface.[5] Subsequently however, the quality of the epitaxy will be impaired by the presence of the plastically deformed region, resulting in a highly defected regrown layer.[16] When implantation does not fully amorphize the layer, good epitaxy is observed.[17] We attribute this to strain levels that are too small to induce plastic deformation. If the implanted layer is thin enough, good regrowth is observed even after full amorphization.[18] We propose that this occurs because for thin layers the yield strain is large,[14] with the result that amorphization occurs before the threshold strain for plastic deformation is reached.

We thank E. Babcock for performing the ion implantation, S. S. Lau for helpful discussions, and L. A. Moudy for technical assistance. This work was supported in part by the Advanced Research Agency of the Department of Defense and was monitored by the Air Force Office of Scientific Research under Contract No. 49620-Tl-C-0087.

[1]L. Csepregi, J. W. Mayer, and T. W. Sigmon, Physics Lett. **54A**, 157 (1975).
[2]L. Csepregi, J. W. Mayer, and T. W. Sigmon, Appl. Phys. Lett. **29**, 92 (1976).
[3]J. W. Mayer, L. Csepregi, J. Gyulai, I. Nagy, G. Mezey, P. Revesz, and E. Kotai, Thin Solid Films **32**, 303 (1976).
[4]K. Gamo, T. Inada, J. W. Mayer, F. H. Eisen, and C. G. Rhodes, Rad. Eff. **33**, 85 (1977).
[5]M. G. Grimaldi, B. M. Paine, M-A. Nicolet, and D. K. Sadana, J. Appl. Phys. **52**, 4038 (1981).
[6]See for example, J. W. Mayer, L. Eriksson, and J. A. Davies, *Ion Implantation in Semiconductors* (Academic, New York, 1970), p. 198.
[7]J. S. Harris, F. H. Eisen, B. Welch, J. D. Haskell, R. D. Pashley, and J. W. Mayer, Appl. Phys. Lett. **21**, 601 (1972).
[8]V. S. Speriosu, J. Appl. Phys. **52**, 6094 (1981).
[9]V. S. Speriosu, B. E. MacNeal, and H. L. Glass, Intermag. 1980 Conf., Boston, paper 22-4 (unpublished).
[10]B. E. MacNeal and V. S. Speriosu, J. Appl. Phys. **52**, 3935 (1981).
[11]E. P. EerNisse, Appl. Phys. Lett. **18**, 581 (1971).
[12]H. Booyens, J. S. Vermask, and G. R. Proto, J. Appl. Phys. **49**, 5435 (1978).
[13]G. A. Rozgonyi, P. M. Petroff, and M. B. Panish, Appl. Phys. Lett. **24**, 251 (1974).
[14]C. A. Ball and C. Laird, Thin Solid Films **41**, 307 (1977).
[15]V. S. Speriosu, B. M. Paine, M.-A. Nicolet, and H. L. Glass (to be published).
[16]S. S. Kular, B. J. Sealy, K. G. Stephans, D. Sadana, and G. R. Booker, Solid-State Electron. **23**, 831 (1980).
[17]J. S. Williams and M. W. Austin, Nucl. Instr. Meth. **168**, 307 (1980).
[18]M. G. Grimaldi, B. M. Paine, M. Maenpaa, M.-A. Nicolet, and D. K. Sadana, Appl. Phys. Lett. **39**, 70 (1981).